Simple Model of Distributed Port (Excitation Source) with Arbitrary Orientation for FDTD Simulations

Nikita Shaimanov
Department of Television and Control
Tomsk State University of Control Systems and Radioelectronics
Tomsk, Russia
nikita.i.shaimanov@tusur.ru

Aleksey Kvasnikov
Department of Television and Control
Tomsk State University of Control Systems and Radioelectronics
Tomsk, Russia
aleksei.a.kvasnikov@tusur.ru

***Abstract*— This paper proposes a simple and versatile distributed port model (a soft-type excitation source) for the standard finite-difference time-domain method. The model represents the port as a thin line formed by a sequence of mesh cell edges. The model allows for arbitrary port orientation, including orientations non-orthogonal to the mesh lines, without significant loss of simulation accuracy. The paper provides a detailed description of the proposed model and its implementation details. Specifically, the paper presents the modified electric field update equations that account for the port internal resistance, the soft-source excitation equation, and the equations for computing the port current and voltage. The model is validated by computing the parameters of an arbitrarily oriented patch antenna and a conformal phased array wrapped around a cylinder. Validation was performed using a custom-developed finite-difference time-domain solver and a commercial solver based on the finite integration technique. The mean relative deviation of the computed parameters was less than 3%, confirming the validity and acceptable accuracy of the proposed model.**

Keywords*— *distributed port, discrete port, excitation source, finite difference time domain method, soft-type source.

I. INTRODUCTION

The finite-difference time-domain (FDTD) method is one of the widely used numerical methods for solving electromagnetics problems [1]. To excite simulated structures such as antennas and microwave devices, FDTD commonly employs ports, categorized into two main types: waveguide ports [2], [3], [4] and discrete ports [5], [6]. Waveguide ports are used to excite structures with a known field distribution, whereas lumped ports are employed when the source needs to be represented as a lumped or distributed element. Among lumped ports, the simplest implementation is the feed gap [7], [8], [9]. In FDTD, this type of port is defined as a one-cell-wide source placed between two conductors or in a gap in a thin wire. The feed gap is simple to implement; however, its accuracy is highly sensitive to the mesh cell size and spatial port orientation. The distributed port overcomes these drawbacks by dividing the excitation amplitude across several mesh cells located within a limited volume. Although implementations of the distributed port for FDTD exist in the literature [10], they are limited to cases where the source is oriented along the coordinate axes. In engineering practice, however, arbitrary (non-orthogonal to the coordinate axes) port placement is often required, for example when simulating wearable electronics, conformal phased arrays, bent microstrip structures, etc. The objective of this paper is to develop a simple and robust distributed port model with arbitrary orientation, suitable for simulating such structures.

The remainder of this paper is organized as follows. Section II describes the proposed distributed port model and its key implementation details. Section III presents the results of the model validation using a patch antenna and a conformal phased array. Section IV describes the results of the work. Section V concludes the paper.

II. DISTRIBUTED PORT MODEL

According to the proposed model, the distributed port is represented as a virtual line defined by two arbitrary user-defined points. The total excitation amplitude and the port internal resistance are distributed among the segments forming this line. Since in FDTD the source current density J_{src} is defined on the edges of Yee cells, the virtual line must align with mesh edges. Consequently, for an arbitrary-oriented distributed port, the line is approximated by a staircase polyline consisting of segments parallel to the coordinate axes.

To obtain this staircase approximation, a greedy algorithm is used to find the shortest path between two points (P_{start} and P_{end}) in a non-uniform mesh. The path selection considers not only cell dimensions but also the distance to the ideal virtual line connecting P_{start} and P_{end}. The output of the algorithm is an ordered set of mesh cell indices corresponding to the x-, y-, and z-directions, along which the excitation is subsequently distributed. Fig. 1 shows the algorithm's operation.

The research was carried out at the expense of Russian Science Foundation grant 23-79-10165, https://rscf.ru/project/23-79-10165/.

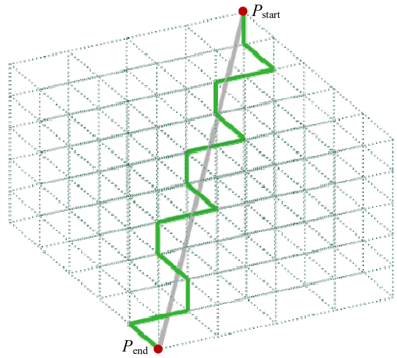

Fig. 1. Example of the greedy algorithm used for the staircase approximation (green) of the ideal virtual line (gray) connecting P_{start} and P_{end}.

As shown in Fig. 2, during the staircase approximation of the port line, short-circuited segments located directly along the conductor boundary can often arise. Including these segments in the distributed port can lead to simulation errors. Therefore, they must be removed. To remove such short-circuited port segments, point-in-polygon algorithms can be used. Alternatively, redundant segments can be filtered based on the values of the electrical conductivity σ assigned to the Yee cell edges intersected by the port.

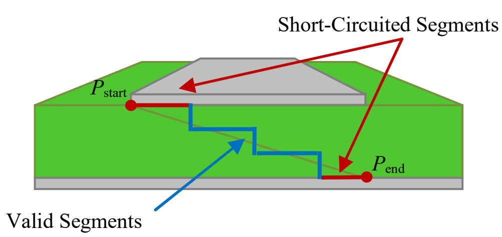

Fig. 2. Example of short-circuited segments (red) arising during the staircase approximation (blue) of the distributed port line.

Following the removal process, the lengths of the remaining segments are summed to compute the total length L of the distributed port. The resulting value of L is then used to distribute the total internal resistance R of the port along its entire length. This is achieved by modifying the coefficients in the finite-difference update equations for the electric field components:

$$E\Big|_{i,j,k}^{n+1} = C1^{(i,j,k)}\, E_y\Big|_{i,j,k}^{n} + C2^{(i,j,k)}\left[\nabla\times \mathrm{H}\Big|_{i,j,k}^{n+\frac{1}{2}}\right] \tag{1}$$

$$C1^{(i,j,k)} = \frac{2\varepsilon_0\, \varepsilon\big|_{i,j,k} - \Delta t\, \sigma\big|_{i,j,k} - \dfrac{L\Delta t}{R\, A\big|_{i,j,k}}}{2\varepsilon_0\, \varepsilon\big|_{i,j,k} + \Delta t\, \sigma\big|_{i,j,k} + \dfrac{L\Delta t}{R\, A\big|_{i,j,k}}}, \tag{2}$$

$$C2^{(i,j,k)} = \frac{2\Delta t}{2\varepsilon_0\, \varepsilon\big|_{i,j,k} + \Delta t\, \sigma\big|_{i,j,k} + \dfrac{L\Delta t}{R\, A\big|_{i,j,k}}}, \tag{3}$$

where Δt is the time step, ε_0 is the vacuum permittivity, ε is the relative permittivity, i, j and k are the spatial indices of the field component, and A is the area of the cell around the port segment.

To excite the distributed port, a time-varying signal $S(t)$ must be applied to all its segments. To minimize reflections at the port location, the excitation is implemented as a soft source [5], [11] by adding the excitation current density J_{exc} to equation (1), as follows:

$$\begin{aligned} E\Big|_{i,j,k}^{n+1} &= E\Big|_{i,j,k}^{n+1} + C2^{(i,j,k)} J_{\text{exc}}^{(i,j,k)} S(t) = \\ &= E\Big|_{i,j,k}^{n+1} + C2^{(i,j,k)} \frac{2V}{R\, A\big|_{i,j,k}} S(t), \end{aligned} \tag{4}$$

where V is the specified peak voltage amplitude at the distributed port.

The resulting characteristics of the distributed port are computed using all of its constituent segments. The total current I^n at the n-th time step is calculated as the arithmetic mean of the currents I_s in each of the S segments along the port line, which, in turn, are determined from the magnetic field components surrounding the segments:

$$I^n = \sum_{s=1}^{S} \frac{I_s^n}{S} = \sum_{s=1}^{S} \frac{\nabla\times H_s^{n+1/2}}{A\big|_{i,j,k}\, S}, \tag{5}$$

The voltage response V^n at the distributed port is computed as the sum of the electric field intensities in each segment multiplied by the lengths L_s of those segments:

$$V^n = \sum_{s=1}^{S} V_s = \sum_{s=1}^{S} E_s^n L_s. \tag{6}$$

III. Model Validation

Validation of the proposed distributed port model has been performed. First, a simple rectangular patch antenna (Fig. 3) rotated by 30° about the z-axis was used as a test structure. The radiating element had dimensions of 30×40×3 mm, and the dielectric substrate with a relative permittivity of $\varepsilon_r = 4$ had dimensions of 60×60×6 mm. Due to the rotation of the structure, the distributed port exciting it was oriented non-orthogonally to the mesh lines. Fig. 4 illustrates the hexahedral discretization of the test structure and the staircase-approximated distributed port line. For the described test structure, the reflection coefficient $|S_{11}|$ and the time-domain voltage response at the port were computed. The results obtained using our FDTD solver and a commercial solver based on the finite integration technique (FIT) [12] with conformal mesh cells were compared.

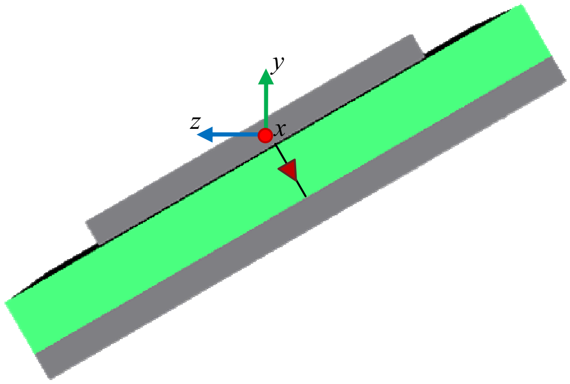

Fig. 3. Test structure of the patch antenna rotated by 30° about the z-axis.

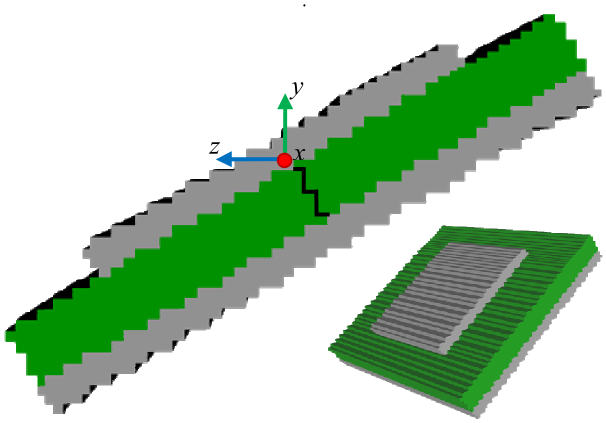

Fig. 4. Discretization of the patch antenna with hexahedral mesh cells. The black line indicates the approximate location of the staircase-approximated line of the distributed port.

The frequency range for $|S_{11}|$ simulation was 0–10 GHz, and the voltage was computed over the interval from 0 to 3.6 ns. A Gaussian pulse was used as the excitation signal $S(t)$, and the mesh step size was $\lambda/55$. A uniaxial perfectly matched layer (UPML) [8] with a thickness of 10 mesh cells was used as the boundary condition. The computed frequency- and time-domain results are shown in Fig. 5 and Fig. 6.

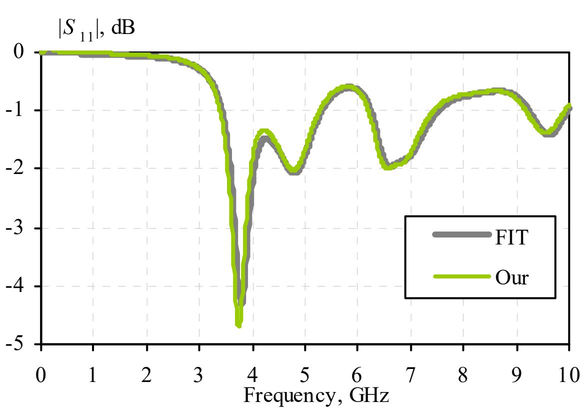

Fig. 5. Frequency dependences of $|S_{11}|$ for the patch antenna with the distributed port, obtained using FIT and our FDTD.

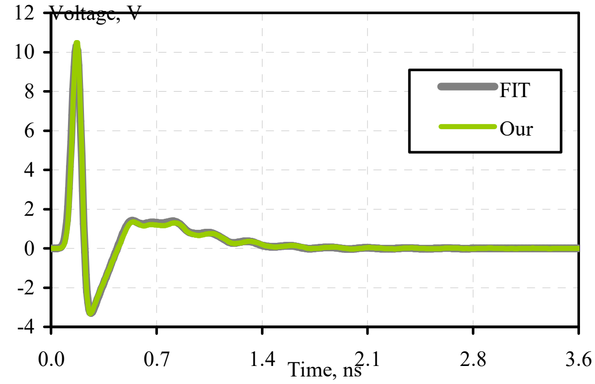

Fig. 6. Time-domain voltage responses at the distributed port of the patch antenna, obtained using FIT and our FDTD.

As shown in Fig. 5 and Fig. 6, the results obtained with the proposed model and those computed by the commercial FIT-based solver are in good agreement. The characteristics exhibit similar behavior and negligibly small differences in the extrema. The mean relative deviation δ between the two frequency dependences of $|S_{11}|$ is only 0.75%. For the time-domain voltage responses, the value of δ is even smaller and does not exceed 0.42%.

Next, a conformal phased array (Fig. 7) consisting of 2×5 patch antenna elements was analyzed using FIT and our FDTD. The elements were square with 10-mm sides and were fabricated on 20×20-mm substrates with $\varepsilon_r = 4$. The phased array was placed around a cylinder with a diameter of 120 mm, meaning that each antenna element was tilted by 20° relative to the previous one. The gap between adjacent elements was set to 1 mm. For validation, the radiation patterns $|E|$ of the phased array at a frequency of 12 GHz were computed and compared. A mesh with a step size of $\lambda/35$ was used. The distributed ports on all antenna elements were set as active with amplitudes of 14.14 V, zero phases, and an internal resistance of 50 Ω. The obtained results are presented in Fig. 8.

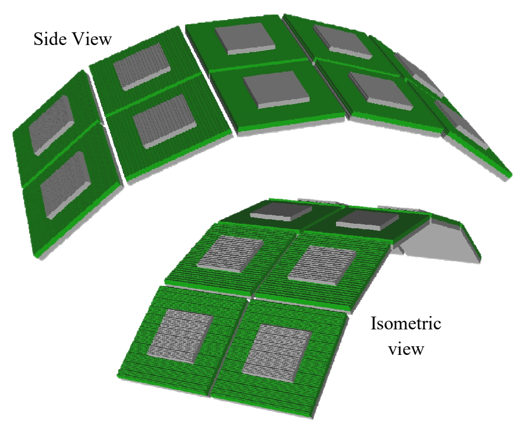

Fig. 7. Test structure in the form of a conformal phased array consisting of 2×5 patch antenna elements.

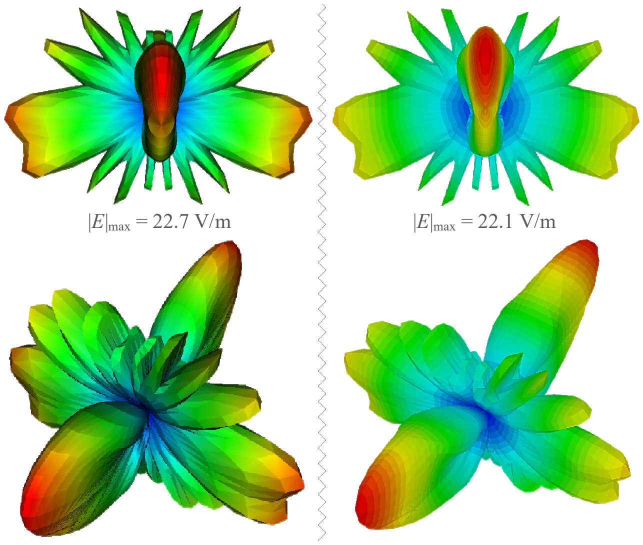

Fig. 8. 3D radiation patterns of the conformal phased array at 12 GHz, obtained using our FDTD (left) and FIT (right).

Fig. 8 shows that the results computed by the commercial FIT-based solver and our FDTD algorithm with the proposed distributed port model are in good agreement. The shapes of the 3D patterns are similar, and the amplitude values of $|E|$ differ by less than 3%. Thus, the obtained results confirm the validity and acceptable accuracy of the proposed distributed port model, as well as its applicability to various electromagnetic problems.

IV. Results

This paper proposes a simple and versatile distributed port model. A description of the model and the key aspects of its implementation in the standard FDTD algorithm is provided. The model has been validated. It was found that the mean deviation between the results obtained using FDTD with this model and those from a commercial FIT-based solver does not exceed 3%. This confirms the validity and acceptable accuracy of the model.

V. Conclusion

The key advantage of the model is the ability to place the port at an arbitrary position and orientation within the computational domain. This enables the simulation of complex structures such as conformal phased arrays, waveguide bends, and microwave devices on flexible substrates without the need to adapt their geometry to the computational mesh. To further improve the accuracy of the model, future work will focus on generalizing it for planar distributed ports with arbitrary orientation.

References

[1] K.S. Yee, "Numerical Solution of Initial Boundary Value Problems Involving Maxwell's Equations in Isotropic Media," IEEE Transactions on Antennas and Propagation, vol. 14, no. 3, pp. 302–307, 1966, doi: 10.1109/TAP.1966.1138693.

[2] Xi Chao Bo, Jian Feng Zhang, and Tie Jun Cui, "Implementation of FDTD Waveguide Port Based on Virtual Domain," in 12th European Conference on Antennas and Propagation, London, UK, pp. 1–3, 2018, doi: 10.1049/cp.2018.0630.

[3] F. Alimenti, P. Mezzanotte, L. Roselli, and R. Sorrentino, "MODAL ABSORPTION IN THE FDTD METHOD: A CRITICAL REVIEW," International Journal of Numerical Modelling: Electronic Networks, Devices and Fields, vol. 10, no. 4, pp. 245–264, 1997, doi: 10.1002/(sici)1099-1204(199707)10:4<245::aid-jnm278>3.0.co;2-p.

[4] F. Alimenti, P. Mezzanotte, L. Roselli and R. Sorrentino, "A revised formulation of modal absorbing and matched modal source boundary conditions for the efficient FDTD analysis of waveguide structures," in IEEE Transactions on Microwave Theory and Techniques, vol. 48, no. 1, pp. 50–59, 2000, doi: 10.1109/22.817471.

[5] A. Taflove and S.C. Hagness, Computational Electrodynamics: The Finite-Difference Time-Domain Method, 3rd ed., Norwood, MA, USA: Artech House, p. 1006, 2005, ISBN: 1580538320.

[6] H.M. Fernandes. Development of Software for antenna analysis and design using FDTD.: Master thesis in Electrical and Computer Engineering, Technical University of Lisbon, p. 114, 2007.

[7] R. Makinen, J. Juntunen and M. Kivikoski, "An accurate 2-D hard-source model for FDTD," in IEEE Microwave and Wireless Components Letters, vol. 11, no. 2, pp. 74–76, 2001, doi: 10.1109/7260.914307.

[8] F. Costen, J. -P. Berenger and A. K. Brown, "Comparison of FDTD Hard Source With FDTD Soft Source and Accuracy Assessment in Debye Media," in IEEE Transactions on Antennas and Propagation, vol. 57, no. 7, pp. 2014–2022, 2009, doi: 10.1109/TAP.2009.2021882.

[9] Veysel Demir, "Formulations for Modeling Voltage Sources with RLC Impedances in the FDTD Method", ACES Journal, vol. 31, no. 09, pp. 1020–1027, 2021.

[10] A.Z. Elsherbeni and V. Demir, The Finite-Difference Time-Domain Method for Electromagnetics with MATLAB Simulations, 2nd ed., Edison, NJ, USA: SciTech Publishing, 2015, ISBN: 1613531753.

[11] D.M. Sullivan, Electromagnetic Simulation Using the FDTD Method, IEEE Press, p. 558, 2000, ISBN: 1118646681.

[12] T. Weiland, "A Discretization Method for the Solution of Maxwell's Equations for Six-Component Fields," in Electronics and Communications, AEU, vol. 31, pp. 116–120, 1977.